

# Poisson's ratios influence on strength and stiffness of cylindrical bars

N. Partaukas\*, J. Bareišis\*\*

\*Kaunas University of Technology, Daukanto 12, 35212 Panevėžys, Lithuania, E-mail: n.partaukas@gmail.com

\*\*Kaunas University of Technology, Daukanto 12, 35212 Panevėžys, Lithuania, E-mail: jonas.bareisis@ktu.lt

**crossref** <http://dx.doi.org/10.5755/j01.mech.17.2.327>

## 1. Introduction

Multi-structural elements (MSE) are made of two or more different materials to withstand the external loads as a solid body. Due to the similarity to composite materials they are often called macro-composites.

Most of MSE's contain better properties than the materials contained in them, for example steel or composite reinforced concrete has higher strength and stiffness [1-5]. MSEs compared with homogeneous structures often have a different nature of fracture, resistance to environmental effects, different stress distribution, etc. Therefore, they are increasingly used not only in construction but also in the water and gas distribution and automotive industry [6-10]. One of the simpler and more often used in engineering practice MSE's is the multilayer bar (MB). There is a wide variety of possible MBs geometries: cylindrical, rectangular bars, pipes, etc. [1, 4, 5].

In combining different materials, it is not only possible to change on the desired direction the strength and stiffness of the MB, but also the costs, surface mechanical and chemical properties, production workability, and so on. For example, polymer, metal or composite layers often protect the MBs from harmful environmental effects [2-4].

When MB's are subjected to tension or compression, this causes uneven stress distribution and their stiffness is different from the composing materials. This phenomenon has long been known and thoroughly studied [11-13]. From the materials mechanical characteristics and bar geometry stresses, effective Young's modulus and strength are calculated. However, most of the techniques are not assessing the Poisson ratios (PR) effect, or simply assume that PR's of the layers are equal.

The most frequently used materials MB's have different PRs. Due to these differences, contact pressure (-es) between layers occur in the cylindrical MB's [14-15] which changes the stress state and the values of axial stress [14-15], stiffness and strength. If the MBs are designed and calculations made according to the methodology [11] or its equivalent, so in case of different PR's this leads to methodological errors.

Poisson's ratio effect on MB's has not yet been thoroughly studied and examined. Paper [15] offers the methodology for the multilayer two-phase rectangular bar stiffness estimation with the account of Poisson effect. The proposed methods in papers [14-15] allow determining the contact pressure and axial stress in case of the two-layer cylindrical bars. However, it remains undetermined to what extent the strength and stiffness of multilayer cylindrical bars are impacted by the Poisson effect.

The aim of this work is to calculate stresses on cylindrical MB's and with regard to Poisson effect, to examine its influence on stress, stiffness and errors produced in case of neglecting this effect.

## 2. Methodology

### 2.1. Bar construction

In this paper we are going to analyze cylindrical MB's, the possible constructions of which are shown in Fig. 3. Material volumetric fractions of 3-layer and 4-layer structures are the same as in 2-layer one. In general, the  $n$ -layer structure may be composed of  $n$  different materials (phases). In further consideration we are going to examine the two-phase MB's with the number of layers between  $2 \leq n \leq 4$ .

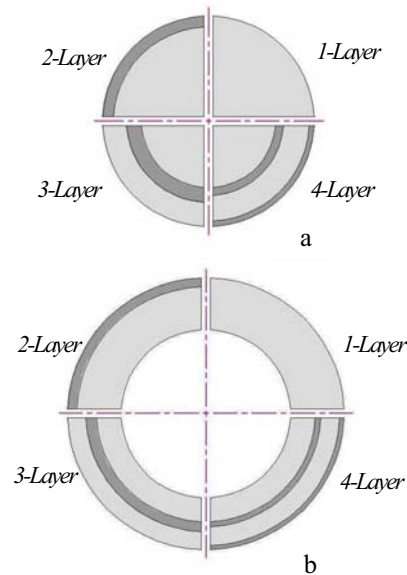


Fig. 1 Cross-section of cylindrical MB's constructions, solid (a) and hollow (b)

### 2.2. N-layer bars

When PR's are the same and there is no contact pressure, the stress state is axial. Then the stresses and effective Young's modulus according to [1] are

$$\sigma'_{z,i} = \frac{F}{A} \frac{E_i}{\sum_{i=1}^n E_i \psi_i} \quad (1)$$

$$E^{eff} = \sum_{i=1}^n E_i \psi_i \quad (2)$$

where  $\sigma'_{z,i}$  axial stress, the  $i$ -th layer,  $F$  and  $A$  are axial load and the general cross-sectional area of the structure,  $E^{eff}$  and  $E_i$  are Young's modulus of the bar (effective) and in the  $i$ -th layer (material),  $\psi_i = A_i A^{-1}$  is the relative

cross-sectional area\* of the  $i$ -th layer.

When PR's are different, there are  $2n-1$  unknowns in the cylindrical bar consisting of  $n$ -layers:  $n$  axial stresses and  $n-1$  contact pressures. All unknowns are obtained when  $2n-1$  equations are formed and solved. The first group of equations is obtained from the condition that all the layers in axial direction deform evenly, i.e. the deformations are equal

$$\varepsilon_{z,i} = \varepsilon_{z,j} \quad (3)$$

The second group of equations are derived from the assumption that the layers are bonded, i.e. their hoop strains in the contact are equal, so

$$\varepsilon_{\theta,i}(\rho_{i,i+1}) = \varepsilon_{\theta,i+1}(\rho_{i,i+1}) \quad (4)$$

where  $\varepsilon_{\theta,i}(\rho_{i,i+1})$  is  $i$ -th layers strain in hoop direction at radius  $\rho_{i,i+1}$  (radius of contact between layers  $i$  and  $i+1$ ).

The last equation is written from static equilibrium

$$\frac{F}{A} = \sum_{j=1}^n \sigma_{z,j} \psi_j \quad (5)$$

Having used Hooke's Law, the deformation equations (3) - (4) are rewritten in terms of stresses. In this way, we obtain  $n$  axial stresses and  $n-1$  equations for the contact pressure. Knowing the stress components, the equivalent stresses (according to von Mises) are found.

MB's stiffness is characterized by the effective elastic modulus ( $E^{eff}$ ). Since the stress state is spatial

$$E^{eff} = \frac{F}{A} \frac{E_i}{\sigma_{z,i} - \nu_i(\sigma_{\theta,i} + \sigma_{r,i})} \quad (6)$$

where  $\sigma_{\theta,i}$  and  $\sigma_{r,i}$  are hoop and radial stress in  $i$ -th layer, respectively.

It is easy to prove that the stress components are directly proportional to the ratio  $F/A$ , so  $E^{eff}$  is independent on it, so it is on radius  $\rho$ , because in that same layer  $\sigma_{\theta,i} + \sigma_{r,i} = Const$ .

It obvious that  $E^{eff}$  can be found if the stresses of at least in one layer are known. As the stress depends on other layers of stiffness,  $E^{eff}$  is a generalized characteristic depending on all the MB's and its layers.

### 2.3. Two-layer bar

The two-layer bar is the simplest case of a multi-layer bar. By applying the equations (4) - (6) for the two-layer bar we obtain the following system of equations:

$$\frac{\sigma_{z,2} - 2p_c \nu_2 \left( \frac{A\psi_1 + \pi r^2}{A(1-\psi_1)} \right)}{\sigma_{z,1} + 2p_c \nu_1 \left( 1 + \frac{\pi r^2}{A\psi_1} \right)} = \xi_{2,1} \quad (7)$$

$$\frac{p_c \left( \frac{A(1+\psi_1) + 2\pi r^2}{A(1-\psi_1)} \right) - \nu_2(\sigma_{z,2} - p_c)}{-p_c \left( 1 + \frac{2\pi r^2}{A\psi_1} \right) - \nu_1(\sigma_{z,1} - p_c)} = \xi_{2,1} \quad (8)$$

$$\sigma_{z,1} \psi_1 + \sigma_{z,2}(1-\psi_1) = \frac{F}{A} \quad (9)$$

where  $p_c$  is contact pressure,  $\nu_i$  is PR of material in  $i$ -th layer,  $\xi_{i+1,i}$  is ratio of Young's modulus in  $i+1$  and  $i$  layers,  $r$  - the internal radius of the bar.

By solving the system of Eqs. (7) - (9), the expressions of contact pressure  $p_c$  and axial stresses  $\sigma_{z,i}$  in the layers can be obtained [13], [14].

From the expression of contact pressure according to Lamé equation radial and hoop stresses of the layers are found. The derivation of the equations (10)-(12) is omitted, because of lack of space, and their analysis and results are presented in the section 'Results and Discussion'.

### 2.4. Three- and four-layer bars

Multi-layer bar can be made from more than two layers. If the bar cross-sectional dimensions are constant, number of the layers increases while their thickness decreases. The increase in the number of layers makes stress expressions more complex, regardless of the number of phases. On the other hand, in this case MB gets more similar to a single composite material than to a structural element. Therefore, the analysis here is narrowed down to four-layered structures.

The analytical expressions of contact pressure between the layers in four-layer case are obtained by solving the system of equations (13) - (19)

$$\frac{\sigma_{z,2} - 2\nu_2 \left( \frac{p_{1,2}\rho_{1,2}^2 - p_{2,3}\rho_{2,3}^2}{\rho_{2,3}^2 - \rho_{1,2}^2} \right)}{\sigma_{z,1} + 2\nu_1 \left( \frac{p_{1,2}\rho_{1,2}^2}{\rho_{1,2}^2 - \rho_{0,1}^2} \right)} = \xi_{2,1} \quad (13)$$

$$\frac{\sigma_{z,3} - 2\nu_3 \left( \frac{p_{2,3}\rho_{2,3}^2 - p_{3,4}\rho_{3,4}^2}{\rho_{3,4}^2 - \rho_{2,3}^2} \right)}{\sigma_{z,2} - 2\nu_2 \left( \frac{p_{1,2}\rho_{1,2}^2 - p_{2,3}\rho_{2,3}^2}{\rho_{2,3}^2 - \rho_{1,2}^2} \right)} = \xi_{3,2} \quad (14)$$

$$\frac{\sigma_{z,4} - 2\nu_4 \left( \frac{p_{3,4}\rho_{3,4}^2}{\rho_{4,5}^2 - \rho_{3,4}^2} \right)}{\sigma_{z,3} - 2\nu_3 \left( \frac{p_{2,3}\rho_{2,3}^2 - p_{3,4}\rho_{3,4}^2}{\rho_{3,4}^2 - \rho_{2,3}^2} \right)} = \xi_{4,3} \quad (15)$$

$$\frac{p_{1,2}\rho_{1,2}^2 - p_{2,3}\rho_{2,3}^2 + (p_{1,2} - p_{2,3})\rho_{2,3}^2}{\rho_{2,3}^2 - \rho_{1,2}^2} + \nu_2(p_{1,2} - \sigma_{z,2})}{\frac{p_{1,2}\rho_{1,2}^2 - p_{1,2}\rho_{0,1}^2}{\rho_{1,2}^2 - \rho_{0,1}^2} + \nu_1(p_{1,2} - \sigma_{z,1})} = \xi_{2,1} \quad (16)$$

\* It shows proportion of the layer cross-sectional area, with respect to the area of bar cross-section (A).

$$\frac{p_{2,3}\rho_{2,3}^2 - p_{3,4}\rho_{3,4}^2 + (p_{2,3} - p_{3,4})\rho_{3,4}^2}{\rho_{2,3}^2 - \rho_{1,2}^2} + v_3(p_{2,3} - \sigma_{z,3})$$

$$\frac{p_{1,2}\rho_{1,2}^2 - p_{2,3}\rho_{2,3}^2 + (p_{1,2} - p_{2,3})\rho_{1,2}^2}{\rho_{2,3}^2 - \rho_{1,2}^2} + v_2(p_{2,3} - \sigma_{z,2}) = \xi_{3,2} \quad (17)$$

$$\frac{p_{3,4}\rho_{3,4}^2 + p_{3,4}\rho_{4,5}^2}{\rho_{4,5}^2 - \rho_{3,4}^2} + v_4(p_{3,4} - \sigma_{z,4})$$

$$\frac{p_{2,3}\rho_{2,3}^2 - p_{3,4}\rho_{3,4}^2 + (p_{2,3} - p_{3,4})\rho_{2,3}^2}{\rho_{2,3}^2 - \rho_{1,2}^2} + v_3(p_{3,4} - \sigma_{z,3}) = \xi_{4,3} \quad (18)$$

$$\sigma_{z,1}\psi_1 + \sigma_{z,2}\psi_2 + \sigma_{z,3}\psi_3 + \sigma_{z,4}\psi_4 = \frac{F}{A} \quad (19)$$

where  $p_{i,j}$  and  $\rho_{i,j}$  are contact pressure between the layers  $i$  and  $j$  respectively, as well as their contact radius.

The contact radius is found from the formula

$$\rho_{i,i+1}^2 = r^2 + \frac{A}{\pi} \sum_{j=1}^i \psi_j \quad (20)$$

For the three-layer bar, the analytical expressions of contact pressure between the layers are derived from the system of equation (13)-(19) having removed equations (15), (18) and restructured equations (14), (17), (19). In both cases the stress components are obtained the same way as for the two-layer bar.

## 2.5. Methodological errors

When the stress state is spatial, one of strength theories has to be applied. We will be using the theory of maximum energy of distortion (von Mises). According to the given methodology, having the stress components  $\sigma_{z,i}$ ,  $\sigma_{\theta,i}$ ,  $\sigma_{r,i}$ , stress intensities  $\sigma_{e,i}$  (von Mises) can be calculated. Stress intensity evaluates strength of the layers taking the Poisson's effect into consideration. The methodological error of [11] is quantitatively found by comparing the axial stresses and stress intensity by the formula

$$\delta_i = \left| \frac{\sigma_{e,i} - \sigma'_{z,i}}{\sigma'_{z,i}} \right| 100 \quad (21)$$

where  $\sigma'_{z,i}$  axial stresses, of the layers according to simplified methodology [11].

The errors of effective Young's modulus, due to the effect of Poisson's, is found by formula similar to (21), using the values given by expressions (2) and (6).

Due to Poisson's effect, the errors of effective Young's modulus are found by the formula similar to formula (21), putting in the values from expressions (2) and (6).

## 3. Results and discussion

### 3.1. Influence on stresses

Firstly, we are going to examine the impact of Poisson's ratios of constituent materials and Young's modulus on the strength two-layer bar. This influence will be quantitative if measured by methodical errors according

to Eq. (21). As an object for study we chose three main two-layer constructions: Metal-Polymer (MP), Metal-Ceramic (MC) and Ceramic-Polymer (CP). In each two-layer bar the material can be arranged in two ways (e.g. M-P and P-M).

The stress errors in constructions MP and PM are shown in Fig. 2, where  $v_M = 0.3$ ,  $v_M = 0.4$ . The continuous lines represent the stiff plastics (e.g. PVC) and soft metal (e.g. aluminium) compositions. The dashed line represents the soft plastic (e.g. PE) and stiff metal (e.g. steel) compositions. When  $E_M = 70 \dots 200$  GPa and  $E_M = 1 \dots 4$  GPa the actual error curves lie between the solid and dashed lines. As shown in Fig. 2, the stress errors of the two-layer M-P bar do not exceed 7.0%.

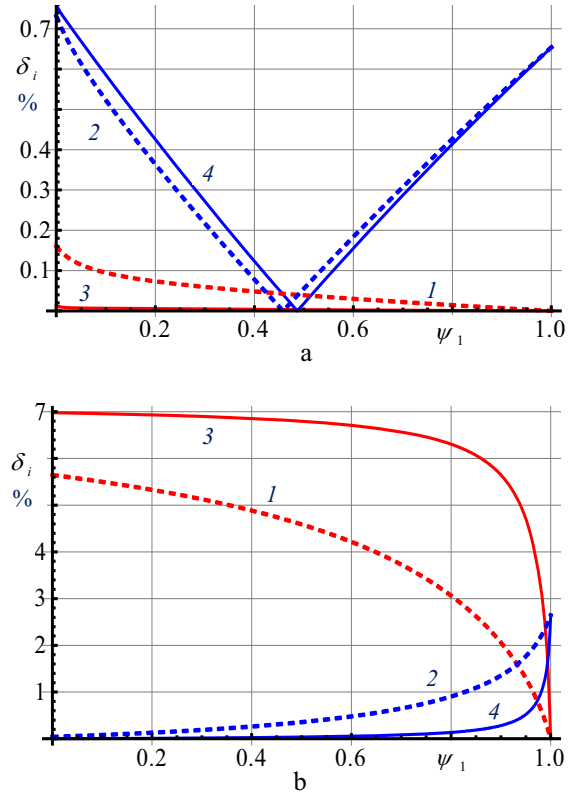


Fig. 2 Stress error dependences on the ratio of cross-sectional areas, when: 1, 2 -  $E_M = 70$  GPa,  $E_P = 4$  GPa; 3, 4 -  $E_M = 200$  GPa,  $E_P = 1$  GPa; 1, 3 stands for internal, and 2, 4 for external layers, a - M-P, b - P-M

In the M-P bar (Fig. 2, a), the error is less than 1.0%, regardless of the Young's modulus. While the errors of P-M bar (Fig. 2, b) increase in one layer, they decrease in the other one. The errors in the polymer layer almost always exceed the metallic ones. The error of metallic layer becomes noticeable only when the layer is thin ( $\psi_2 < 10\%$ ). The more different Young's modulus, the lower are the errors in the metals and higher in the polymers. When the bar is hollow, the errors are similar, except for the case when the hole diameter is small. Due the stress concentration, the stress error of the polymer layer may reach up to 11%. The errors of the metallic layer, due to this reason, practically are not affected.

The errors of stress in the M-P construction cannot be taken into account and it is considered that in such cases the methodology [1] present rather accurate results.

Regarding P-M constructions the methodology [1] and similar to them should be applied with caution, because the actual stresses in the polymer layer may be very different from the calculated ones.

Ceramic-Metal (C-M, M-C) compositions due to their high strength and low cost are widely used in construction. The variations of the stress errors are shown in Fig. 3. In case of the MC construction the errors of the metallic layer reach up to 3.5% (Fig. 3, a), and around 2% in the CM construction (see Fig. 3, b). The maximum error (about 6%) is obtained in the ceramic layer, with the CM arrangement of solid bar construction, as ceramics is less rigid than metal, and its volumetric ratio is low. In case of the hollow construction the maximum values of the errors are smaller but similar.

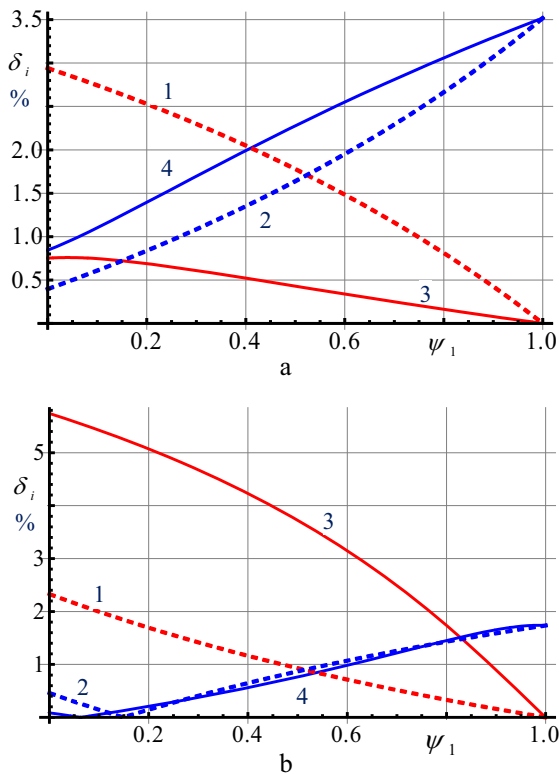


Fig. 3 Stress error dependences on ratio of cross-sectional areas, when: 1, 2 -  $E_M = 70$  GPa,  $E_C = 100$  GPa; 3, 4 -  $E_M = 200$  GPa,  $E_C = 50$  GPa; 1, 3 stands for internal, and 2, 4 for external layers, a - M-C, b - C-M

Thus, in most cases the errors of the ceramic-metal structures are about 1-3%. The layer arrangement does not affect the stress in the cardinal way, contrary to the polymer-metal structure (compare Fig. 3 and Fig. 2). When high precision is not required, in the most cases these errors can be ignored and considered that the stress state is uni-axial, as methodology [1] claims.

The Ceramic-Polymer composition is less widely used (Fig. 4). The errors in such bars have similar character as in the polymer-metal bars, except that their values are much higher (Fig. 2). High stress errors (up to 14.0%) occurred at the polymer layer in the P-C bar. If the bar is hollow, the error is highly dependent on the radius  $r$ . The smaller the radius the higher the error (may be up 46.5%). The Error decreases with increasing radius and becomes lower than those at solid bars.

Larger errors in the C-P composition are obtained

in a polymer layer (up to 3.0%), but only in case of its significant volumetric ratio. Thus, in case of the C-P construction the stress errors can be considered as negligible, however, this cannot be stated of the of the PC case. The stress state of the following bar is in mismatch with those presented by the methodology [1]. This is because of higher difference of Poisson's ratios, as the error variation of P-C and P-M bars is similar in their nature, only their values are different (compare Fig. 2 and Fig. 4).

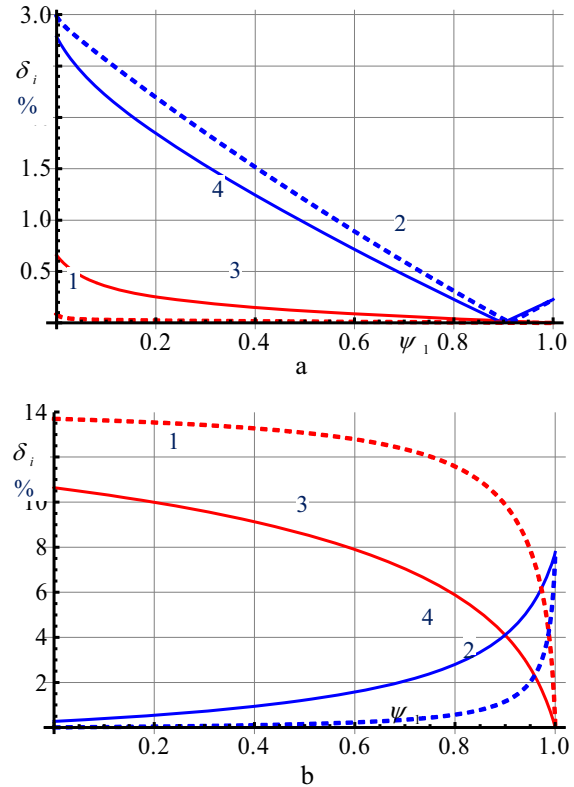


Fig. 4 Stress error dependences on ratio of cross-sectional areas, when: 1, 2 -  $E_C = 100$  GPa,  $E_P = 1$  GPa; 3, 4 -  $E_C = 50$  GPa,  $E_P = 4$  GPa; 1, 3 stands for internal, and 2, 4 for external layers, a - C-P, b - P-C

It should be noted that the results have been obtained on the assumption that the deformations are elastic and any fracture or flow processes are absent. The value of the stresses can also change due to the layer delimitation (lost adhesion between the layers).

### 3.2. Influence on stiffness

One of important characteristics of the multi-layer bar (MB) is stiffness or effective Young's modulus. Its value, as seen in the formula (6), depends on stress state of the layers. When the stress state is axial, the modulus  $E_K$  [1] calculated using the formula (2), will be different from the effective modulus  $E^{eff}$  calculated by (6). This causes the stiffness error in a multi-layer bars.

It has been obtained that the error of stiffness depends on geometry of the bar. When the Poisson's ratios  $\nu_1 = 0.5$ ,  $\nu_2 = 0.2$ , in a hollow bar, the error of stiffness is about 1- 4% (Fig. 5, b). In case of a solid bar, the error is much higher (up to 8%, see Fig. 5, a). In both cases, the error depends on the ratios  $\psi_1$ ,  $\xi_{2,1}$ .

A really significant effect on the values of stiff-

Table 1

Stress errors of solid multilayer bars

| Geometry  | Properties  | n | Stress error, % |       |         |
|---|---|---|-----------------|-------|---------|
|   |   |   | P-M             | P-M-P | P-M-P-M |
| $D_I^* = 0.0$ mm,<br>$D_E^* = 26.0$ mm,<br>$\psi_P = 0.8, \psi_M = 0.2$ | $E_P = 1.0$ GPa<br>$E_M = 200.0$ GPa<br>$\nu_P = 0.4, \nu_M = 0.3$  | 1 | 6.31            | 6.61  | 6.89    |
|   |   | 2 | 0.14            | 0.07  | 0.05    |
|   |   | 3 | -               | 0.29  | 4.66    |
|   |   | 4 | -               | -     | 0.30    |
|   |   |   | C-M             | C-M-C | C-M-C-M |
| $D_I = 0.0$ mm,<br>$D_E = 26.0$ mm,<br>$\psi_C = 0.1, \psi_M = 0.9$     | $E_C = 50.0$ GPa<br>$E_M = 200.0$ GPa<br>$\nu_C = 0.2, \nu_M = 0.3$ | 1 | 5.42            | 5.54  | 5.66    |
|   |   | 2 | 0.05            | 0.00  | 0.03    |
|   |   | 3 | -               | 1.51  | 3.51    |
|   |   | 4 | -               | -     | 0.18    |
|   |   |   | P-C             | P-C-P | P-C-P-C |
| $D_I = 0.0$ mm,<br>$D_E = 26.0$ mm,<br>$\psi_P = 0.2, \psi_C = 0.8$     | $E_P = 1.0$ GPa<br>$E_C = 100.0$ GPa<br>$\nu_P = 0.4, \nu_C = 0.2$  | 1 | 13.54           | 13.61 | 14.08   |
|   |   | 2 | 0.04            | 0.03  | 0.21    |
|   |   | 3 | -               | 0.57  | 7.56    |
|   |   | 4 | -               | -     | 0.28    |

Table 2

Stress errors of hollow multilayer bars

| Geometry   | Properties  | n | Values of stress errors, % |       |         |
|--|---|---|----------------------------|-------|---------|
|  |   |   | P-M                        | P-M-P | P-M-P-M |
| $D_I = 21.0$ mm,<br>$D_E = 34.0$ mm,<br>$\psi_P = 0.8, \psi_M = 0.2$ | $E_P = 1.0$ GPa<br>$E_M = 200.0$ GPa<br>$\nu_P = 0.4, \nu_M = 0.3$  | 1 | 0.44                       | 0.62  | 0.60    |
|  |   | 2 | 0.05                       | 0.02  | 0.14    |
|  |   | 3 | -                          | 0.38  | 2.17    |
|  |   | 4 | -                          | -     | 0.23    |
|  |   |   | C-M                        | C-M-C | C-M-C-M |
| $D_I = 21.0$ mm,<br>$D_E = 34.0$ mm,<br>$\psi_C = 0.1, \psi_M = 0.9$ | $E_C = 50.0$ GPa<br>$E_M = 200.0$ GPa<br>$\nu_C = 0.2, \nu_M = 0.3$ | 1 | 3.64                       | 3.55  | 3.58    |
|  |   | 2 | 0.09                       | 0.07  | 0.05    |
|  |   | 3 | -                          | 1.96  | 3.43    |
|  |   | 4 | -                          | -     | 0.12    |
|  |   |   | P-C                        | P-C-P | P-C-P-C |
| $D_I = 21.0$ mm,<br>$D_E = 34.0$ mm,<br>$\psi_P = 0.2, \psi_C = 0.8$ | $E_P = 1.0$ GPa<br>$E_C = 100.0$ GPa<br>$\nu_P = 0.4, \nu_C = 0.2$  | 1 | 0.37                       | 0.04  | 0.11    |
|  |   | 2 | 0.01                       | 0.01  | 0.16    |
|  |   | 3 | -                          | 0.58  | 2.33    |
|  |   | 4 | -                          | -     | 0.18    |

\*  $D_I, D_E$  mark the inner and outer diameter of the bar respectively, n represents numbers of the layers.

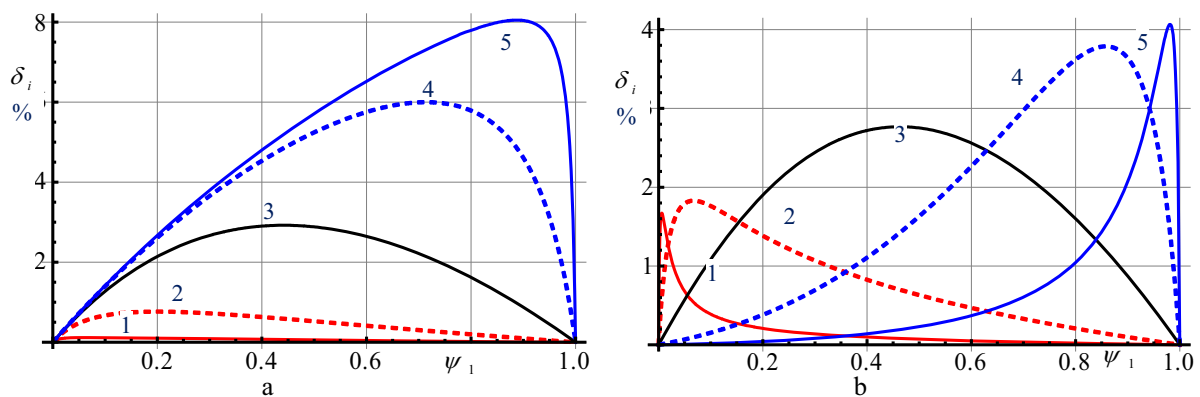


Fig. 5 Stiffness errors dependence on ratios of cross-sectional areas and Young's modulus, when: 1 -  $\xi_{2,1} = 0.01$ , 2 -  $\xi_{2,1} = 0.1$ , 3 -  $\xi_{2,1} = 1$ , 4 -  $\xi_{2,1} = 10$ , 5 -  $\xi_{2,1} = 100$   $\nu_1 = 0.5, \nu_2 = 0.2$ , a – solid, b – hollow

ness errors are created by Poisson's ratio. When  $\nu_1 = 0.4, \nu_2 = 0.3$ , the error of the solid bar reaches up to 0.5%, while in the hollow one just 0.3% respectively. When the differences of Poisson's ratios are constant, the error of stiffness will be higher if one layer has a ratio closer to 0.5, i.e. when one of the materials is incompressible.

The larger the difference between Poisson's ratios, the higher is the contact pressure between the layers; and the methodology [1], assuming that the contact pressure is absent presents more and more inaccurate results. The fact that solid bar presents higher errors may be explained by the fact that a solid layer resists deformation more than a hollow one. The hollow layer can deform in the direction

of the hole, while the solid one only by changing its volume.

From the data presented it is clear that the error of stiffness does not only depend on the bar type, but also on the values of relative cross-sectional area of the layers, Young's modulus and Poisson's ratios (Fig. 5). When  $|\nu_2 - \nu_1| < 0.3$  and  $\xi_{2,1} < 10$ , the errors are negligibly small and formula (2) gives the exact value of effective Young's modulus. Theoretically, the error of stiffness may reach 25%. Such errors are obtained when  $\xi_{2,1} \rightarrow \infty$ ,  $\nu_2 \rightarrow 0$ ,  $\nu_1 \rightarrow 0.5$  and  $\psi_1 \rightarrow 1$ .

The maximum stress error of 36.4 % is obtained in the inner layer of the solid bar, when  $\nu_1 \approx 0.1$ ,  $\nu_2 \approx 0.5$ ,  $\xi_{2,1} \rightarrow \infty$ . Extremely high errors are obtained in the hollow bar at the inner layer if the inner radius is very small. Then, according to the methodology [1], the stresses can differ from the actual ones several times.

The maximum stress error of the outer layer is 21.3%. It is obtained when  $\nu_1 \approx 0.5$ ,  $\nu_2 \approx 0.1$ ,  $\xi_{2,1} \rightarrow 0$ . The error in it has only an insignificant dependence on whether the inner layer is hollow or solid.

As for the stiffness errors, the stress errors are highly dependent on the difference of Poisson's ratios. When  $|\nu_2 - \nu_1| < 0.1$  regardless of the values of Young's modulus, bar geometry and the layer layout the stress error will not exceed 7.2%. In these cases, the approximate methodology [1] can be applied. When the difference is higher, the errors of stress and stiffness may become more significant. In such cases, we recommend to use the methodology here presented instead of [11].

### 3.3. Multilayer bar

After the analysis of the two-layer bars it remains to examine the multilayer bars ( $i > 2$ ). To determine values of the error equations (13) - (21) were used. For further study we chose the cases where the highest errors in the two-layer bar were obtained (see Fig. 2-4). The subject was a multi-layer bar with 3 and 4 layers, composed of two different materials (phases). The volumetric ratio of the Phases in 2, 3 and 4-layer bars was equal. The results are presented in Tables 1 and 2.

While analysing the impact of the layer number on the stress errors it is clear that the increase in the number of the layers causes the increase of errors in inner layers, rather insignificantly though. It should be noted that moving from the two-layer to the three- of four-layer bar, the stress errors of the inner and outer layers of the same material are significantly different (see table 1). In Tables 1 and 2 a trend is seen that the closer the layer is to the bar surface the lower are the errors, and vice versa.

Moving from two-layers to the three or four layers in the hollow bars, the stress error may be increased (Table 2). Results presented (Tables 1 and 2) clearly show that the stress errors in the two-layer bar can be used for an approximate estimation of the multilayer bar error. In other words, instead of the complex 3-layer or 4-layer equations, simpler 2-layer bar equations (6) - (12) can be used. Increasing the number of the layers has little impact on stiffness of the bar.

## 4. Conclusions

Due to Poisson's effect contact pressure appears in the axially loaded multilayer bars. The bar strength, stresses and stiffness are affected as a result. A mathematical model for this pressure, equivalent stresses and bar stiffness calculation in the cylindrical multi-layer bar, with estimation of the influence of Poisson's effect is proposed. The equations derived were used to determine the stress and stiffness errors that occur in case this effect is neglected.

Stress and stiffness error variations for the two-phase bars made of two, three or four layers have been determined. It was obtained that when the difference of Poisson's ratios is 0.1 or greater, then the strength and stiffness errors may become significant. In such cases the effect of Poisson's effect cannot be neglected.

Strength and stiffness errors also depend on Young's modulus, cross-sectional areas (i.e. volumetric ratios of the phases), geometry and the layers of the layout. The errors of solid bars are usually greater than those of the hollow ones. Stiffness errors are usually much lower than the ones of the stress.

Large errors are obtained in polymer-metal solid bar construction when the polymer lies inside the bar and within polymer-ceramic structures. In metal-ceramic and polymer-metal constructions, when the polymer is outside the bar, and regardless of the layout of the layers, the stress and stiffness errors are negligible.

After the examination of three and four layer two-phase bars and comparison with the two-layer construction it was obtained that an increased number of the layers usually has no significant effect on the errors. The errors of multilayer bars may be both larger and smaller than the two-layer ones. This depends on the layer thickness and arrangement: the inner layers of the bar tend to increase in errors, while in contrast, the outer layers tend to decrease.

The stiffness errors in the two- and multi-layer bars are very similar. In our view, the stress and especially stiffness of multi-layer bars can be rather accurately estimated from a similar two-layer construction. In other words, equations (6) - (12) may be used for the multi-layer bar strength and stiffness evaluation. The relative advantage of the two-layer model compared with the multi-layer model is that it contains simpler expressions in analytical formulas.

It is not only Poisson's effect that can cause stress and stiffness errors, but also the change in temperature, creep of the material, etc. Thus, the total amount of errors of the multi-layer bar may be higher than has been shown here.

## References

1. **Li, G.; Torres, S.; Alaywan, W.; Abadie, C.** 2005. Experimental study of fip tube-encased concrete columns. *Journal of Composite Materials* 39: 1131.
2. **Salloum, Y.A.; Almusalim, T.H.** 2005. Load capacity of concrete masonry block walls strengthened with epoxy-bonded GFRP sheets, *Journal of Composite Materials* 39: 1719-1745.
3. **Valivonis, J.; Skuturna, T.** 2007. Cracking and strength of reinforced concrete structures in flexure strengthened with carbon fibre laminates, *Journal of*

- Civil Engineering and Management 4: 317-323.
4. **Kuranovas, A.; Kvedaras, A.K.** 2007. Behaviour of hollow concrete-filled steel tubular composite elements, *Journal of Civil Engineering and Management* 2: 131-141.
  5. **Li, G.; Maricherla, D.** 2007. Advanced grid stiffened fiber reinforced plastic tube encased concrete cylinders, *Journal of Composite Materials* 41: 1803.
  6. **Wang, X.; Li, M.D.; et al.** 2001. Self-strengthening research of fiber reinforced pressure vessel with metallic liners, *Journal of Reinforced Plastics and Composites* 16: 1390-1413.
  7. **Ivanov, S.G.; Strikovskii, L.L.; et al.** 2005. Modeling the mechanical behavior of metal-reinforced thermoplastic pipes under internal pressure, *Mechanics of Composite Materials* 1: 57-70.
  8. **Kobayashi, S.; Imai, T.; Wakayama, S.** 2007. Burst strength evaluation of the FW-CFRP hybrid composite pipes considering plastic deformation of the liner, *Composites: Part A* 38: 1344-1353.
  9. **Lees, J.M.** 2006. Behaviour of GFRP adhesive pipe joints subjected to pressure and axial loadings, *Composites: Part A* 37: 1171-1179.
  10. **Hausding, J.; et al.** 2006. Compression-loaded multilayer composite tubes, *Composite Structures* 76: 47-51.
  11. **Bareišis, J.** 2004. Design and stress state of tensions in multilayer bars, *Journal of Composite Materials* 5: 389-393.
  12. **Bareišis, J.; Kleiza, V.** 2004. Research in the limiting efficiency of plastic deformation of multilayer tension (compression) bars, *Mechanics of Composite Materials* 2: 135-144.
  13. **Partaukas, N.; Bareišis, J.** 2009. The stress state in two-layer hollow cylindrical bars, *Mechanika* 1(75): 5-12.
  14. **Partaukas, N.; Bareišis, J.** 2009. The stress state in two-layer solid cylindrical bars. *Mechanika-2009, Proceedings of the 14th International Conference*: 301-306.
  15. **Liu, B.; Feng, X.; Zhang, S.** 2009. The effective Young's modulus of composites beyond the Voigt estimation due to the Poisson effect, *Composites Science and Technology* 13: 2198-2204.
  16. **Shariati, M.; et al.** 2010. Numerical and experimental investigation on ultimate strength of cracked cylindrical shells subjected to combined loading, *Mechanika* 4(84): 12-19.

N. Partaukas, J. Bareišis

#### PUASONO KOEFICIENTO ĮTAKA CILINDRINIŲ STRYPŲ STIPRUMUI IR STANDUMUI

R e z i u m ė

Tempiant (gniuždant) daugiasluoksnius strypus, dėl skirtingų Puasono koeficiento verčių tarp sluoksnių atsiranda kontaktinis slėgis. Dėl to sluoksniuose susidaro erdvinis (triais) įtempių būvis. Darbe pasiūlyta analitinė metodika, įgalinanti tiksliai apskaičiuoti įtempius, atsižvelgiant į Puasono koeficientų įtaką. Juos ignoruojant, atsiranda įtempių ir standumo skaičiavimo paklaidos. Straipsnyje nagrinėjama, nuo ko priklauso ir kaip kinta dvisluoksnių ir daugiasluoksnių cilindrinų strypų įtempių ir standumo paklaidos.

N. Partaukas, J. Bareišis

#### POISSON'S RATIOS INFLUENCE TO CYLINDRICAL BARS STRENGTH AND STIFFNESS

S u m m a r y

In case Multilayer cylindrical bars are subjected to tension or compression, due to Poisson effect, contact pressure between the layers occurs. As a result, a spatial stress state arises in the material. The analytical methodology for accurate determination of stresses, assessing the influence of this effect is proposed. In case this phenomenon is neglected, this often leads to stress, strength and stiffness methodological errors. The paper examines in detail how big they are and how these errors change in multilayer cylindrical bars. In addition to this, analytical equations to obtain the stress in multilayer bars are presented, at the same time evaluating the influence of Poisson effect.

Н. Партаукас, Й. Барейшис

#### ВЛИЯНИЕ КОЭФФИЦИЕНТА ПУАССОНА НА ПРОЧНОСТЬ И ЖЕСТКОСТЬ ЦИЛИНДРИЧЕСКИХ СТЕРЖНЕЙ

Р е з ю м е

При растяжении-сжатии многослойных стержней из-за разных значений коэффициента Пуассона создается контактное давление между слоями. Из-за этого в слоях образуется объемное (трехосное) напряженное состояние. В работе предложена аналитическая методика, позволяющая точно определить напряжения с учетом влияния коэффициентов Пуассона. Игнорирование последних ведет к погрешностям расчета прочности и жесткости. Анализируется, от чего зависит и как меняются погрешности прочности и жесткости как в двухслойных, так и в многослойных цилиндрических стержнях.

Received October 12, 2010  
Accepted April 07, 2011